Diabetes, Metabolic Syndrome and Obesity: Targets and Therapy Dovepress
open access to scientific and medical research

Open Access Full Text Article

ORIGINAL RESEARCH

Qihu Preparation Ameliorates Diabetes by Activating the AMPK Signaling Pathway in db/db Mice

Hongfang Zeng[1–3,*]
Xiaoli Li[1–3,*]
Duanfang Zhou[1–3]
Ning Wang[4]
Xiaoping Yu[1–3]
Liangyuan Long[1,3]
Hao Cheng[5,6]
Shuyu Zhou[5]
Zhengze Shen[7]
Weiying Zhou[1–3]

[1]Department of Pharmacology, College of Pharmacy, Chongqing Medical University, Chongqing, People's Republic of China; [2]Chongqing Key Laboratory of Drug Metabolism, Chongqing, People's Republic of China; [3]Key Laboratory for Biochemistry and Molecular Pharmacology of Chongqing, Chongqing, People's Republic of China; [4]West China Biopharm Research Institute, West China Hospital, Chengdu, Sichuan Province, 610041, People's Republic of China; [5]China Company 18th, College of Pharmacy, Army Medical University, Chongqing, 400038, People's Republic of China; [6]Department of Pharmacy, Medical Security Center, the 925 Hospital, Joint Logistic Support Force, Guiyang, Guizhou Province, 550005, People's Republic of China; [7]Department of Pharmacy, Yongchuan Hospital Affiliated to Chongqing Medical University, Chongqing, 400016, People's Republic of China

*These authors contributed equally to this work

Correspondence: Weiying Zhou
Department of Pharmacology, College of Pharmacy, Chongqing Medical University, 1 Yixueyuan Road, Yuzhong District, Chongqing, 400016, People's Republic of China
Tel/Fax +86 23 684 85161
Email wyzhou0118@163.com

Purpose: To examine the pharmacological effects of Qihu on type 2 diabetes mellitus using db/db mice.

Materials and Methods: Thirty-seven db/db mice were randomly divided into the following 5 groups: diabetes model control group (DM group; n = 7), administered with the adjuvant 0.3% carboxymethyl cellulose-Na; positive control group (Met group; n = 8), administered with metformin (0.13 g/kg bodyweight); Qihu-L group (n = 7), administered with a low dose of Qihu (0.75 g/kg bodyweight), Qihu-M group (n = 7), administered with a medium dose of Qihu (1.5 g/kg bodyweight); Qihu-H group (n = 8), administered with a high dose of Qihu (3.0 g/kg bodyweight). BKS mice (n = 8) were used as the negative control group. The db/db mice were administered with drugs through oral gavage for 28 days. The random blood glucose levels, glucose tolerance test, bodyweight, food intake, and blood lipid levels of the mice were measured during the experimental period. The liver and pancreas tissues were collected for pathological, quantitative real-time polymerase chain reaction, and Western blotting analyses.

Results: Compared with the DM group, the Qihu groups exhibited decreased bodyweight gain. The blood glucose levels in the Qihu-L, Qihu-M, and Qihu-H were 31.46%, 43.73%, and 51.83%, respectively, lower than those in the DM group. The triglyceride levels were significantly downregulated and the swelling and steatosis of the hepatocytes were significantly lower in the Qihu-M and Qihu-H groups than in the DM group. Qihu downregulated the expression of IL-1β, IL-6, and TXNIP and upregulated the AMP-activated protein kinase (AMPK) signaling pathway in the pancreas and liver tissues of db/db mice.

Conclusion: The anti-diabetic effects of Qihu are mediated through the activation of the AMPK/Txnip signaling and the downregulation of the secretion of inflammatory factors in db/db mice.

Keywords: type 2 diabetes mellitus, T2DM, Traditional Chinese medicine, TCM, TXNIP, anti-inflammatory

Introduction

In addition to energy metabolism dysregulation, the metabolic syndrome type 2 diabetes mellitus (T2DM) is associated with chronic inflammation. According to the latest data released by the International Diabetes Federation, 425 million individuals were diagnosed with diabetes in 2017 worldwide with an average incidence of 1 case in every 11 adults and approximately 5 million diabetes-related deaths.[1] T2DM mainly manifests as metabolic disorders characterized by hyperglycemia, hyperlipidemia, and insulin resistance.[2] Chronic dysregulation of glucose

Received: 21 March 2021
Accepted: 2 July 2021
Published: 14 July 2021

metabolism can result in serious health complications and lead to various organ pathologies, such as diabetic retinopathy, diabetic nephropathy, and diabetic neuropathy. Additionally, these complications contribute to diabetes-associated death.

The major drugs currently used to treat T2DM are sulfonylureas, biguanides, α-glucosidase inhibitors, and thiazolidinediones. However, these drugs do not efficiently regulate blood glucose levels and are associated with various side effects, such as cardiovascular toxicities and gastrointestinal discomforts. Traditional Chinese medicine (TCM) can treat some complex diseases, including diabetes.[3–5] Therefore, the development of safe and effective TCM-based treatment for diabetes has piqued the interest of Chinese medicine practitioners.

The Qihu preparation (Qihu) comprises more than 10 natural products, including *Panax notoginseng* (Burkill) F. H. Chen ex C. H. (Araliaceae), *Dendrobium nobile* Lindl., Gen. Sp. Orchid. Pl. (Orchidaceae), *Astragalus membranaceus* Moench, Methodus (Moench) (Leguminosae), and *Pueraria lobata* (Willd) Ohwi. (Fabaceae). According to the Compendium of Materia Medica, *P. notoginseng* and *D. nobile* can be used to treat diabetes. Consistently, several studies have demonstrated the anti-diabetic effects of *P. notoginseng* and *D. nobile*.[6,7] Recent studies have reported that *P. notoginseng* and *D. nobile* exhibit glucose-lowering, lipid-lowering, anti-inflammatory, and antioxidant activities.[8,9] According to the principles of TCM, *D. nobile* alleviates metabolic disturbances by replenishing yin for maintaining gastric tonicity, promoting body fluid production, nourishing yin, and clearing heat.[10] Additionally, Zhang et al reported that *P. notoginseng* exerts anti-obesity effects by downregulating lipid synthesis, inhibiting adipogenesis, and upregulating energy consumption.[11] Yang et al demonstrated that *P. notoginseng* can attenuate lung cancer growth partly by modulating the Met/miR-222 axis.[12] Hu et al reported that *P. notoginseng* attenuates the lipopolysaccharide-induced blood-brain barrier disruption and monocyte adhesion to cerebral endothelial cells in vitro by activating the Nrf2 antioxidant defense system through a PI3K/Akt-dependent mechanism and inhibiting the NF-κB inflammatory signaling pathway.[13] He et al demonstrated that *D. nobile* exhibits immune-modulatory activities by stimulating the production of cytokines (tumor necrosis factor (TNF)-α and interleukin (IL)-1β) in cells.[14] Additionally, *D. nobile* is reported to exert therapeutic effects on depression, colon cancer, and ethanol-induced gastric mucosal injury.[15–17] As Qihu contains *P. notoginseng* and *D. nobile*, it can be a potential preventive and therapeutic agent for diabetes and its complications.

Previously, we had demonstrated that Qihu can effectively decrease the blood glucose levels in KK-Ay mice.[18] However, the pharmacological effects and the underlying mechanisms of Qihu have not been elucidated. This study aimed to examine the pharmacological effects and mechanism of Qihu in db/db mice to promote the clinical development and application of Qihu.

Materials and Methods

Qualitative Phytochemical Analysis

High-performance liquid chromatography (HPLC) coupled to electron source ionization (ESI) and quadrupole time-of-flight mass spectrometry (Q-TOF-MS) (HPLC-ESI-TOF-MS) analysis was performed to qualitatively analyze the main phytochemical components of Qihu. The samples were injected into a Waters BEH C18 (2.1 × 100 mm i.d.; 1.7 μm, Waters, Massachusetts, USA) column at 45°C using a gradient elution at a flow rate of 1.0 mL/min. The mobile phase comprised 0.1% formic acid-water (A) and methanol (B). The gradient program was as follows: 0–5 min, 5% B; 5–10 min, 5–20% B; 8–12 min, 20–25% B; 12–16 min, 25–30% B; 16–20 min, 30–40% B; 20–25 min, 40–60% B; 25–30 min, 60–70% B. The flow rate was maintained at 0.25 mL/min and the sample injection volume was 2 μL. All MS experiments were performed using a triple quadrupole mass spectrometer equipped with an ESI interface. Nitrogen was used as both the auxiliary and sheath gases with a flow rate of 12 L/min. The MS analysis was performed in negative scan mode under the following conditions: dry gas temperature, 320°C; fragmentor voltage, 100 V; nebulizer pressure, 45 psi. Full scan data acquisition and dependent scan event data acquisition were performed from m/z 100 to 1000. The quality deviations of Qihu were within 5 ppm. At the concentration range of 1–500 μg/L, a good linear relationship was observed with the correlation coefficients of more than 0.99. The retention time deviations were less than 0.2%. The limit of detection of the instrument was 0.5–20 μg/L, while the limit of quantification was 1–50 μg/L. The analysis was completed within 40 min. The detection sensitivity, resolution, and reproducibility satisfied the detection requirements.

Drugs and Reagents

Qihu was provided by Qihu Biopharmaceutical (Chongqing, China). These Chinese herbal medicines were blended in a specific ratio in a three-dimensional

mixer of SBH-200 series for 30 min and granulated using a rocking granulator (YK-160 type) after powdering. The wet granules were placed in a hot air circulation drying oven (Model TX-881-0) and dried at a constant temperature of 55 ± 2°C for 4.5–5 h until the moisture content of the material was ≤ 10%. The dried granules were placed in a ZS-350 vibrating screen and granulated through an 18-mesh sieve to obtain the preparation.

Metformin hydrochloride was purchased from Squibb (Shanghai, China). Sodium carboxymethyl cellulose (CMC-Na) was provided by Aladdin (Shanghai, China). Blood glucometer and blood glucose test strip were obtained from Johnson & Johnson (Shanghai, China). The Trizol kits were purchased from TaKaRa (Dalian, China). The reverse transcription and quantitative real-time polymerase chain reaction (qRT-PCR) kits were obtained from Bimake (Houston, Texas, USA). Bicinchoninic acid (BCA) protein assay kit and sodium dodecyl sulfate-polyacrylamide gel electrophoresis (SDS-PAGE) precast gels were purchased from Beyotime (Shanghai, China). The anti-AMP-activated protein kinase (AMPK), anti-p-AMPK, anti-TXNIP, and anti-β-actin antibodies (Supplemental Table S1) were purchased from Cell Signaling Technology (Beverly, MA, USA). The horseradish peroxidase-conjugated secondary antibodies were purchased from Zhongshan Jinqiao (Beijing, China). The enzyme-linked immunosorbent assay (ELISA) kits for IL-1β and IL-6 were provided by ThermoFisher (New York, USA).

Experimental Animals

Thirty-seven BKS-Leprem2Cd479/Nju (db/db) and eight C57BLKS/JNju (BKS) mice (aged 5–6 weeks with a bodyweight of 15–30 g; males and females in equal ratio) were purchased from the Nanjing University Model Animal Research Institute. The animals had free access to qualified sterilized feed, which was supplied twice a week, and sterilized tap water in a water bottle. Additionally, the animals were maintained in a controlled environment under the following conditions: temperature, 21°C–24°C (daily temperature difference was not more than 4°C); humidity, 35%–72%; circadian conditions; 12-h light/dark cycle. The number of air changes in the room was not less than 10 times/h.

Animal Experiments

The animal experiments were performed according to the National Guidelines for Animal Care and Use and were approved by the Animal Care and Use Committee of Chongqing Medical University. BKS mice were used as the negative control group (NC; n = 8), which was intragastrically administered with 0.3% CMC-Na. The db/db mice that satisfied the diagnostic criteria for diabetes (random blood glucose ≥11.1 mmol/L) were randomly divided into the following 5 groups according to the blood glucose level and bodyweight: diabetes model control group (DM group; n = 7), intragastrically administered with 0.3% CMC-Na; positive control group (Met group; n = 8), intragastrically administered with metformin hydrochloride (0.13 g/kg bodyweight); Qihu low-dose group (Qihu-L group; n = 7), intragastrically administered with a low dose of Qihu (0.75 g/kg bodyweight); Qihu medium-dose group (Qihu-M group, n = 7), intragastrically administered with a medium dose of Qihu (1.5 g/kg bodyweight); Qihu high-dose group (Qihu-H group, n = 8), intragastrically administered with a high dose of Qihu (3.00 g/kg bodyweight). The drugs were administered twice a day at an interval of more than 4 h for 28 days.

Observation Indices

The observation indices, including the behavior, health status, hair, and death, were recorded during the experimental period. The food intake was measured for three consecutive days every week for 4 weeks and the average food intake per animal was calculated. The bodyweight and random blood glucose (RBG) levels were monitored once a week. Additionally, the glucose tolerance test (GTT) was performed after 4 weeks administration. The mice were fasted for 12 h of the next day with free access to drinking water. The blood glucose were recorded before the mice were intraperitoneally injected with 10% D-glucose (1.0 g/kg bodyweight). Blood glucose levels were measured at 30, 60, 120 and 180 min.

Blood Lipid Level Determination and Histopathological Examination

At the end of the experiment, the mice were anesthetized and the blood samples were obtained from the eyeball and stored at 4°C for 2 h. Next, the blood samples were centrifuged at 3000 g for 20 min. The serum was used to determine the lipid levels. The liver and pancreas were excised and rinsed with cold physiological saline. Some hepatic tissues were fixed with 4% paraformaldehyde, embedded in paraffin, and stained with hematoxylin and eosin.

qRT-PCR

Total RNA was isolated from the pancreas and liver tissues using the Trizol kit, following the manufacturers' instructions. The RNA was dissolved in diethylpyrocarbonate-treated water. The quality of the RNA was determined based on the ratio of optical density at 260 nm to that at 280 nm using a NanoDrop ONE spectrophotometer (NanoDrop Technologies, Wilmington, DE). The RNA was reverse-transcribed into complementary DNA using the reverse transcription kit (All-in-One cDNA Synthesis SuperMix from Bimake), following the manufacturer's instructions. The PCR was performed using 2x SYBR Green qPCR Master Mix and the conditions were as follows: 95°C for 4 min (Hot-Start DNA polymerase activation), followed by 39 cycles of 95°C for 20 s (denaturation), 66°C for 10 s (annealing), and 70°C for 10 s (extension), and a final extension at 70°C for 10 s. PCR was performed using a BioRad CFX Connect Real-Time PCR instrument (BioRad, Hercules, CA). The primers used for qRT-PCR analysis are shown in Table 1. The expression levels of the target genes were normalized to those of β-actin (housekeeping gene). The data were analyzed using the $2^{-\Delta\Delta Ct}$ method [ΔCt = Ct (target gene) − Ct (housekeeping gene); ΔΔCt = ΔCt (experimental group) − ΔCt (control group)].

Table 1 Sequences of Primers Used in qRT-PCR

Genes		Sequences
IL-1β	F	AGTTGACGGACCCCAAA
	R	TCTTGTTGATGTGCTGCTG
IL-6	F	TTCACAAGTCGGAGGCTTA
	R	CAAGTGCATCATCGTTGTTC
TXNIP	F	CGGACGGGTAATAGTGGA
	R	TGTGTCTTCATAGCGCAAG

Abbreviations: F, forward primer; R, reverse primer.

ELISA

The levels of IL-1β and IL-6 in the liver and pancreas homogenates were measured using commercial kits, following the manufacturers' instructions.

Western Blotting

The tissues were homogenized and the total proteins were extracted in radioimmunoprecipitation lysis buffer (Beyotime Biotechnology, Shanghai, China) containing 1% phenylmethylsulfonyl fluoride. The proteins were quantified using the BCA protein assay kit (Beyotime Biotechnology, Shanghai, China). Western blotting was performed as previously described.[19] Briefly, the proteins were subjected to SDS-PAGE using a 10% gel. The resolved proteins were transferred to a polyvinylidene difluoride membrane (Millipore, Shanghai, China). The membrane was blocked with 5% skimmed milk or bovine serum albumin for 2 h at room temperature and incubated with primary antibodies overnight at 4°C. Next, the membrane was washed thrice with Tris-buffered saline with Tween 20 (TBST) and incubated with secondary antibodies for 2 h at room temperature. After washing thrice with TBST, the membrane was incubated with SuperSignal Chemiluminescent substrate (UltraSignal ECL Reagent, 4 A Biotech Co., Ltd, China). The protein bands were visualized using the Image Lab detection system (BioRad, Hercules, CA).

Statistical Analysis

All data are expressed as mean ± standard deviation. The data were analyzed using with Student's *t*-test using GraphPad Prism 6.0 software (GraphPad, Inc., Chicago, IL, USA). The differences were considered significant at $p < 0.05$.

Results

Phytochemical Analysis of Qihu

To qualitatively investigate the main phytochemical constituents of Qihu, HPLC-ESI-Q-TOF-MS analysis was performed. More than 20 major constituent peaks were detected within 30 min in the HPLC chromatogram of Qihu (Figure 1A). The following eight main components were identified through comparison with our established formula data of the known chemical constituents of Qihu (Table 2): quercetin, ferulic acid, dendrobine, sophoradiol, gigantol, naringin, notoginsenoside R1, and ginsenoside Rb1 (Figure 1B). The mass spectrum of eight main components was shown in supplemental data Figures S1-S8.

Effects of Qihu on Food Intake and Bodyweight in Db/Db Mice

Compared with that in the NC group, the average food intake was significantly higher in the DM group in all 4 weeks ($p < 0.01$) (Figure 2A). This was consistent with the characteristics of db/db mice. The food intake in the Qihu-M and Qihu-H groups was significantly lower than that in the DM group in weeks 2 and 3 ($p < 0.05$ or $p < 0.01$). In week 4, the food intake in the Qihu-M and Qihu-H groups was obviously lower than that in the DM group but there was no statistical difference.

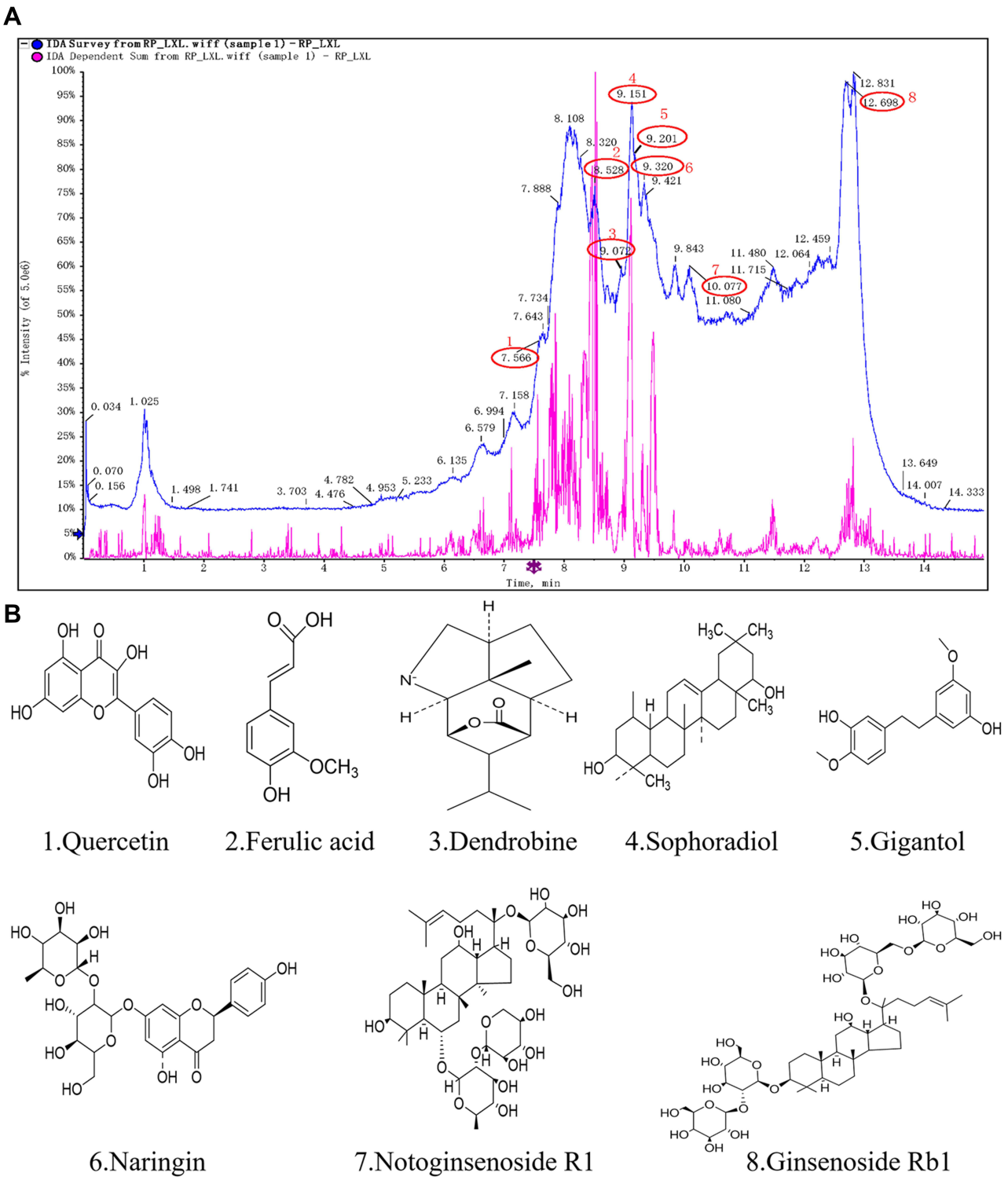

Figure 1 The results of the HPLC-ESI-Q-TOF analysis of Qihu. The results of the HPLC-ESI-Q-TOF analysis of Qihu. (**A**) The main components chemical structures of Qihu were 1. *Quercetin*, 2. *Ferulic acid*, 3. *Dendrobine*, 4. *Sophoradiol*, 5. *Gigantol*, 6. *Naringin*, 7. *Notoginsenoside R1*, and 8. *Ginsenoside Rb1*. (**B**) All of these compounds are the main ingredients of *Panax notoginseng, Dendrobium nobile, Astragalus membranaceus* and *Pueraria lobata*, etc.

Compared with that in the DM group, the food intake was decreased in the Qihu-L, Qihu-M, and Qihu-H groups in weeks 1 and 2, and the difference became smaller in weeks 3 and 4. In addition the food intake in the Met group was significantly lower than that in the DM group only in week 2 ($p < 0.05$).

Table 2 Main Components of Qihu

NO.	Formula	Mass (Da)	Extraction Mass (Da)	Found At Mass (Da)	Error (ppm)	Found At RT (min)	RT Delta (min)	RT % Error
1	$C_{15}H_{10}O_7$	302.04265	303.04993	303.04987	−0.2	7.4	7.4	0
2	$C_{10}H_{10}O_4$	194.05791	195.06519	195.06531	0.6	8.95	8.95	0
3	$C_{16}H_{25}NO_2$	263.18853	264.19581	264.19484	−3.7	9.07	9.07	0
4	$C_{30}H_{50}O_2$	442.38108	443.38836	443.38846	0.2	9.15	9.15	0
5	$C_{16}H_{18}O_4$	274.12051	275.12779	275.12661	−4.3	9.2	9.2	0
6	$C_{27}H_{32}O_{14}$	580.17921	581.18648	581.18833	3.2	9.33	9.33	0
7	$C_{47}H_{80}O_{18}$	932.53447	933.54174	933.54173	0	10.02	10.02	0
8	$C_{54}H_{92}O_{23}$	1108.60294	1109.61022	1109.60802	−2	12.68	12.68	0

The bodyweight of mice was monitored once a week (Figure 2B). In the NC group, the bodyweight remained low and slowly increased during the experimental period. The bodyweight of the DM group was two times higher than that of the NC group and continued to increase during the experimental period. Treatment with metformin slightly mitigated the bodyweight gain in db/db mice. The bodyweight of the Qihu-L, Qihu-M, and Qihu-H groups was significantly lower than that of the DM group from day 15 to day 29 ($p < 0.01$). On day 29, the bodyweights of the DM, Met, Qihu-L, Qihu-M, and Qihu-H groups were 45.35 ± 2.37, 42.12 ± 3.96, 40.67 ± 2.92, 38.80 ± 3.12, and 34.84 ± 3.96 g, respectively.

Effects of Qihu on the Levels of Random Blood Glucose, Glucose Tolerance and Blood Lipids

The blood glucose levels in the DM group were more than 11.1 mmol/L during the experimental period, which was the diagnostic criteria for diabetes and consistent with the characteristics of the T2DM model. As shown in Figure 3A, the random blood glucose level in the Qihu-M and Qihu-H groups was significantly lower than that in the DM group from day 8 ($p < 0.05$ or $p < 0.01$). Compared with those in the DM group, the random blood glucose levels were significantly lower in the Met group from day 15 ($p < 0.01$). Additionally, the blood glucose level in the Qihu-L group was significantly lower than that in the DM group from day 22 ($p < 0.05$). Qihu dose-dependently decreased the random blood glucose level in db/db mice. The hypoglycemic effect of the medium dose of Qihu was similar to that of metformin. However, the hypoglycemic effect of the high dose of Qihu was slightly better than that of metformin. This indicated that Qihu exerts a potent anti-hyperglycemic effect in db/db mice.

As shown in Figure 3B, the GTT was performed in mice after 4 weeks of Qihu treatment. Compared with the

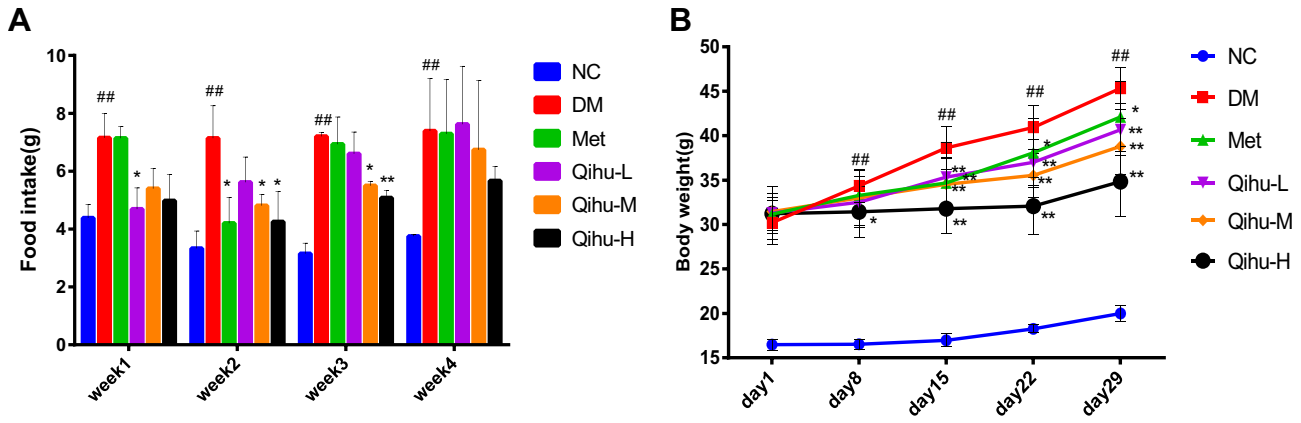

Figure 2 The effects of Met and Qihu on food intake and body weight in db/db mice. The db/db mice were treated with 0.3% sodium carboxymethyl cellulose (CMC-Na, used as DM control), Met or different doses of Qihu as described in methods. BKS mice were used as the negative control group, which was intragastrically administered with 0.3% CMC-Na. (**A**) The food intake was measured for 3 consecutive days every week for 4 weeks, and then the average food intake per animal was calculated. (**B**) The body weight was monitored once a week. All data were expressed as mean ± SD (n = 7–8). $^{\#\#}p < 0.01$ vs NC, $^{*}p < 0.05$ or $^{**}p < 0.01$ vs DM.

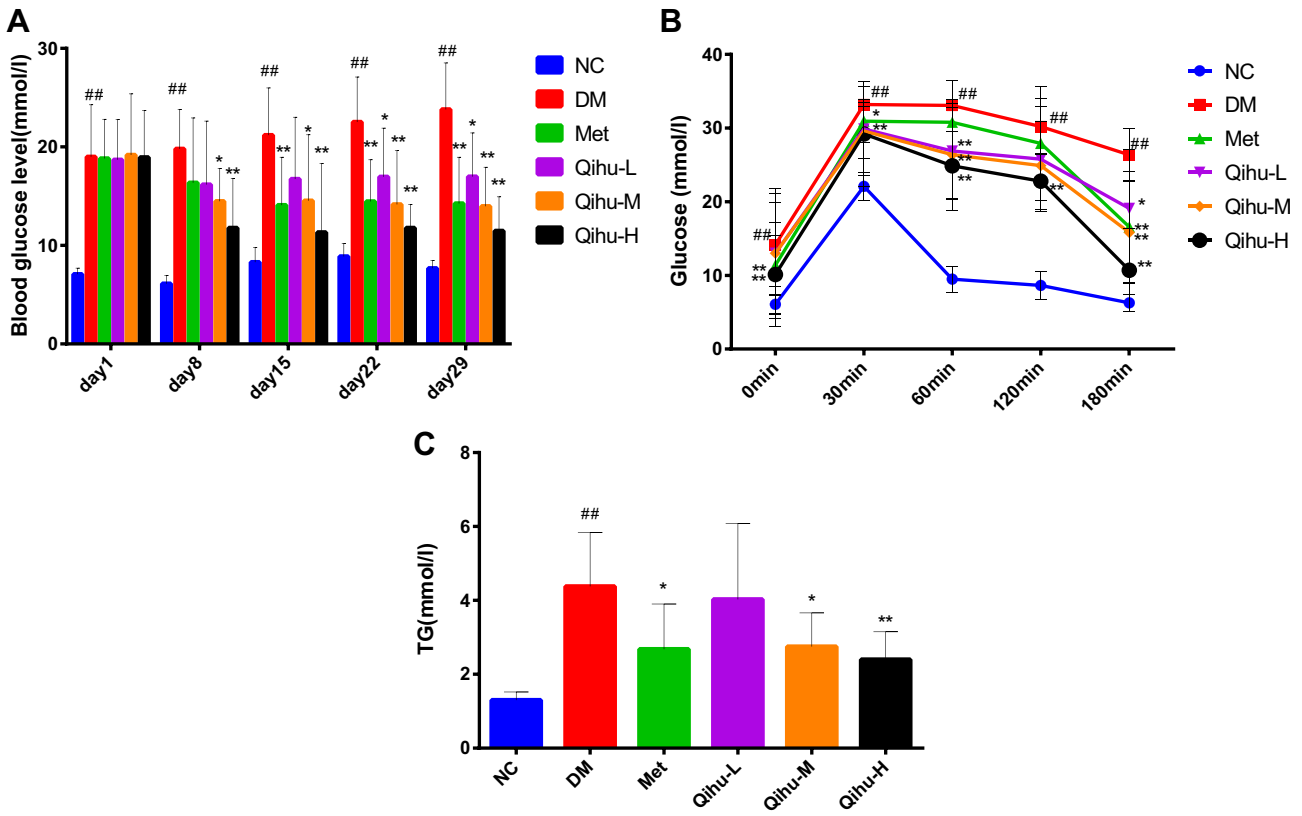

Figure 3 The effects of Met and Qihu on the levels of blood glucose and TG in db/db mice. (**A**) The effects of Met and Qihu on the levels of blood glucose in db/db mice. The blood glucose levels were monitored once a week. (**B**) The effect of Met and Qihu on glucose tolerance in db/db mice. (**C**) The effect of Met and Qihu on TG levels in db/db mice. All data were expressed as mean ± SD (n = 7–8). $^{\#}p < 0.05$ or $^{\#\#}p < 0.01$ vs NC, $^{*}p < 0.05$ or $^{**}p < 0.01$ vs DM.

NC group, the blood glucose levels of the DM group were significantly higher than that of the NC group at all time points ($p < 0.01$). Compared with the DM group, the blood glucose levels of the Qihu-H group were significantly lower than that of the DM group from the time point of 60-minute ($p < 0.01$). In addition, at the time point of 180-minute, the blood glucose levels of all the administration groups were significantly lower than that of the DM group ($p < 0.05$ or $p < 0.01$).

The effect of Qihu on blood triglyceride (TG) levels is shown in Figure 3C. Compared with those in the NC group (1.30 ± 0.22 mmol/L of NC), the TG levels were significantly higher in the DM group (4.38 ± 1.45 mmol/L) ($p < 0.01$). The TG levels in the Met group were 38.81% lower than those in the DM group. Additionally, the TG levels were significantly downregulated in the Qihu-M (2.75 ± 0.91 mmol/L) and Qihu-H (2.40 ± 0.75 mmol/L) groups ($p < 0.05$ vs DM). In contrast, the levels of total cholesterol, high-density lipoprotein, and low-density lipoprotein were not significantly different between the Qihu-L, Qihu-M, Qihu-H, and DM groups (data not shown).

Effects of Qihu on the Histopathological Changes in the Liver

The liver specimens of mice from different groups were subjected to histopathological analyses. The histopathological damage was scored according to the criteria described in Table 3. In the NC group, the hepatocytes exhibited regular arrangement. The pathological score of the liver section of the NC group was grade 0 (Figure 4A and B). The hepatocytes of the DM group exhibited disordered arrangement, swelling, and steatosis. The pathological score of the liver sections of the DM group was grade 2 or grade 3. The NC and DM groups exhibited significantly different pathological scores ($p < 0.01$). The swelling and steatosis of the hepatocytes in the Met, Qihu-M, and Qihu-H groups

Table 3 Pathological Scoring Criteria of Liver

Scoring Criteri	Pathological Grade
Hepatocyte cord structure disappears, hepatocytes swell and steatosis occurs. Obvious fat deposition can be observed	3
Hepatic cell swelling and steatosis are alleviated	2
Hepatocytes have basically returned to normal size and steatosis has basically Disappeared	1
Hepatocytes are densely packed, without swelling and steatosis	0

were significantly alleviated when compared with those in the DM group. The average pathological scores of the liver sections from the Met, Qihu-M, and Qihu-H groups were 2, 2, and 1, respectively.

Effects of Qihu on the Expression Levels of IL-1β and IL-6

Inflammation contributes to the pathogenesis of T2DM. The effect of Qihu on the expression levels of IL-1β and IL-6 in db/db mice is shown in Figure 5. The mRNA levels of IL-1β and IL-6 in the pancreas and liver tissues of the DM group were significantly higher than those in the pancreas and liver tissues of the NC group. Compared with those in the pancreas and liver tissues of the DM group, the mRNA levels of IL-1β and IL-6 were downregulated in the pancreas and liver tissues of the Qihu-L, Qihu-M, Qihu-H, and Met groups (Figure 5A–D). This suggests that Met and Qihu downregulate the mRNA levels of IL-1β and IL-6 in the pancreas and liver tissues of db/db mice. Consistently, the results of ELISA revealed that the protein expression levels of IL-1β and IL-6 in the pancreas and liver tissues of the Qihu-L, Qihu-M, Qihu-H, and Met groups were significantly lower than those in the pancreas and liver tissues of the DM group ($p < 0.01$) (Figure 5E–H).

Effects of Qihu on AMPK Signaling and TXNIP Expression

AMPK and TXNIP play critical roles in insulin resistance, inflammation, and regulation of glucose levels in diabetes.[20–23] The effect of Qihu on AMPK signaling and TXNIP expression was examined in this study (Figure 6A–D). Qihu increased AMPK phosphorylation and decreased TXNIP mRNA and protein levels in a dose-dependent manner in pancreas and liver tissues of db/db mice.

Discussion

Diabetes, a metabolic disorder, is caused by insufficient insulin secretion and/or insulin resistance. In addition to inducing systemic changes, diabetes can result in fatal complications in humans. The key strategy to treat diabetes is to control hyperglycemia and prevent diabetes-associated complications. TCM has a long history of treating diabetes, which was first recorded in Shennong's Materia Medica. The natural characteristics and mild and long-lasting efficacy, especially in the prevention and control of chronic complications of diabetes, are major advantages of TCM for improving the quality of life of patients. Therefore, the application of TCM for the treatment of diabetes has piqued the interest of the scientific community.[24–26]

Recent studies have demonstrated that *D. nobile* and *P. notoginseng* have various pharmacological activities, such as alleviating skeletal muscle insulin resistance and anti-glycemic and anti-lipidemic activities in db/db mice.[27,28] The db/db mice harbors a mutation in the leptin receptor-encoding gene located on chromosome 4, which results in the induction of diabetes. This spontaneous diabetes model has been recommended for examining the pharmacodynamics of hypoglycemic drugs by the Ministry of Health in the "Guide to Research on New Drugs in Traditional Chinese Medicine." The pathogenesis of diabetes in db/db mice is similar to that in patients with T2DM. The db/db mice are associated with bulimia and obesity at 4 weeks of age. Additionally, the blood glucose and lipid levels increase with age in db/db mice. In this study, the blood glucose levels in the DM group were 11.1 mmol/L. Additionally, the bodyweight of the DM group gradually increased during the experimental period. Qihu significantly downregulated the blood glucose levels and mitigated the increased bodyweight gain and food intake in db/db mice. Glycosylated hemoglobin (GHb) can effectively indicate glycemic control in the past 2–3 months in patients with diabetes. Hence, GHb, which is the gold standard for determining glycemic control, is a critical biomarker for diagnosing and managing diabetes. Treatment with Qihu or metformin did not markedly decrease the GHb levels (data not shown), which may be attributed to the short treatment duration (1 month).

Diabetes is accompanied by dysregulated lipid metabolism and susceptibility to complications, such as

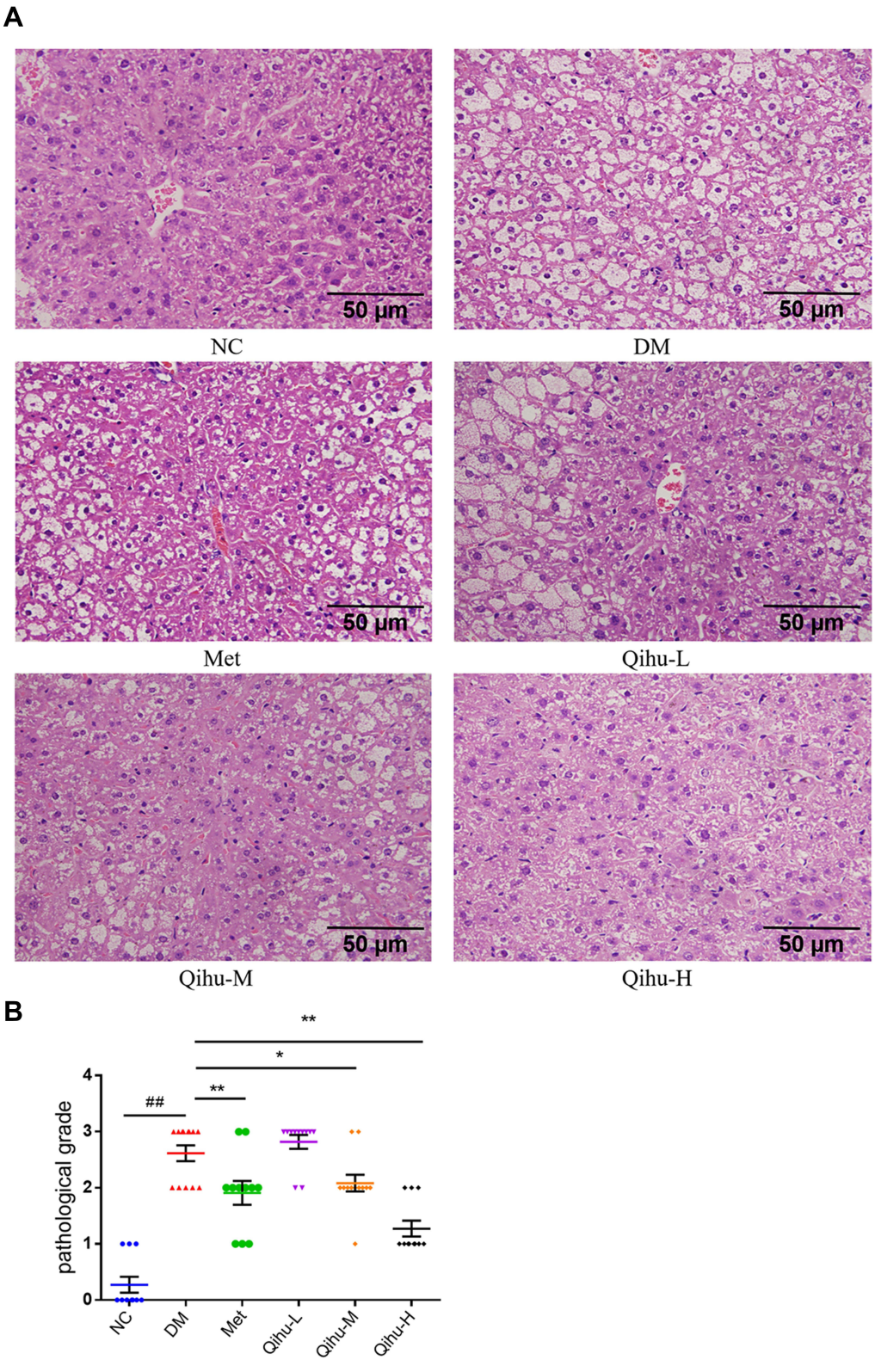

Figure 4 The effect of Met and Qihu on the pathological changes of liver in db/db mice. (**A**) The effect of Met and Qihu on the pathological changes of liver in db/db mice. The liver was excised from db/db mice and part of the tissues was fixed with 4% paraformaldehyde, and then embedded in paraffin and stained with hematoxylin and eosin (magnification: ×400). (**B**) The result of pathological score in all the groups of mice. All data were expressed as mean ± SD (n = 7–8). $^{\#\#}p < 0.01$ vs NC, $^{*}p < 0.05$ or $^{**}p < 0.01$ vs DM.

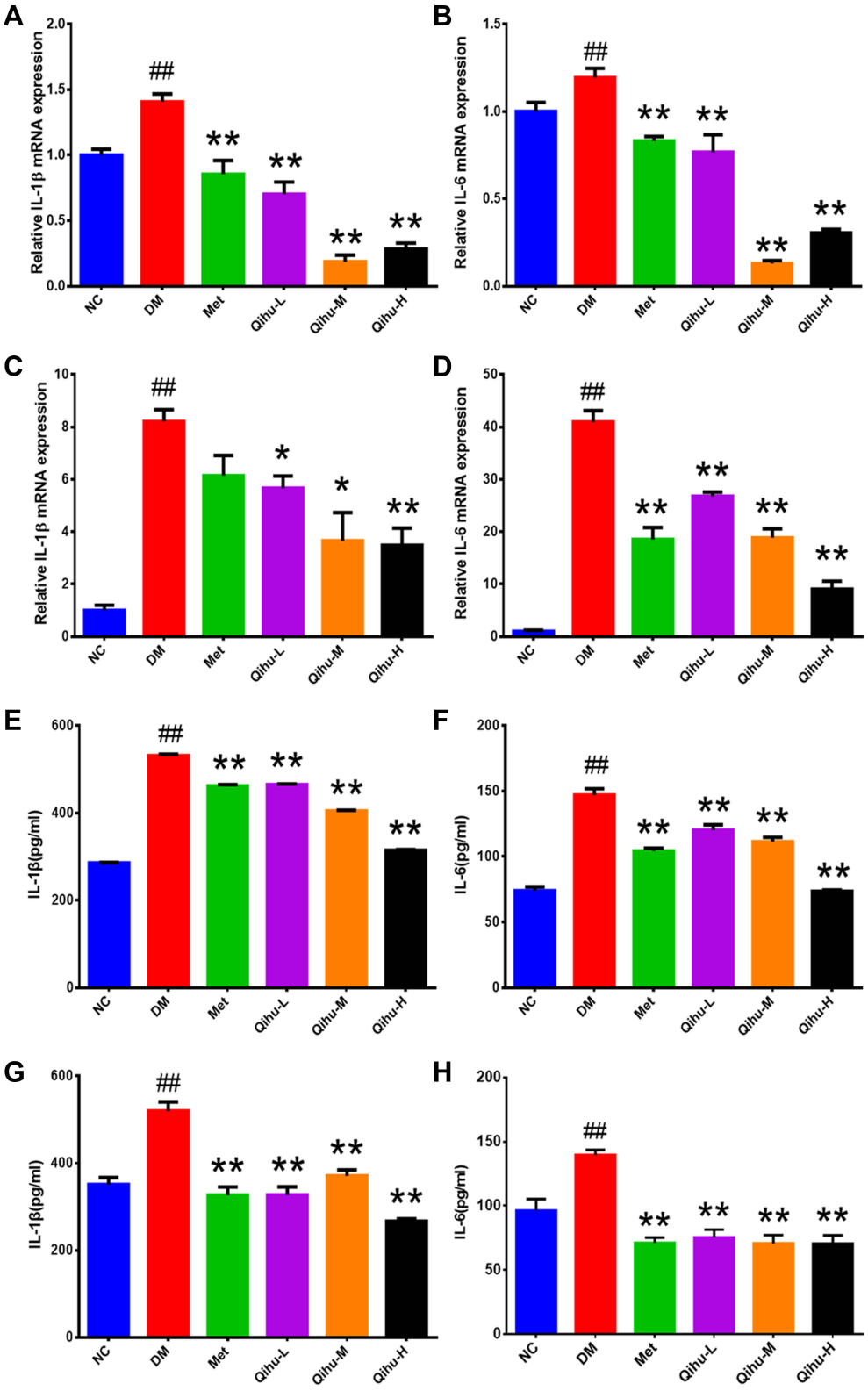

Figure 5 The effect of Qihu on the expression levels of IL-1β and IL-6 in the liver and pancreas of db/db mice. (**A**–**D**) The IL-1β and IL-6 mRNA levels in liver (**A** and **B**) and pancreas (**C** and **D**) were detected using qRT-PCR assay. (**E** and **F**) The IL-1β and IL-6 protein levels in the liver (**E** and **F**) and pancreas (**G** and **H**) were detected using ELISA analysis. All data were expressed as mean ± SD (n = 3). $^{\#\#}p < 0.01$ vs NC, $^{*}p < 0.05$ or $^{**}p < 0.01$ vs DM.

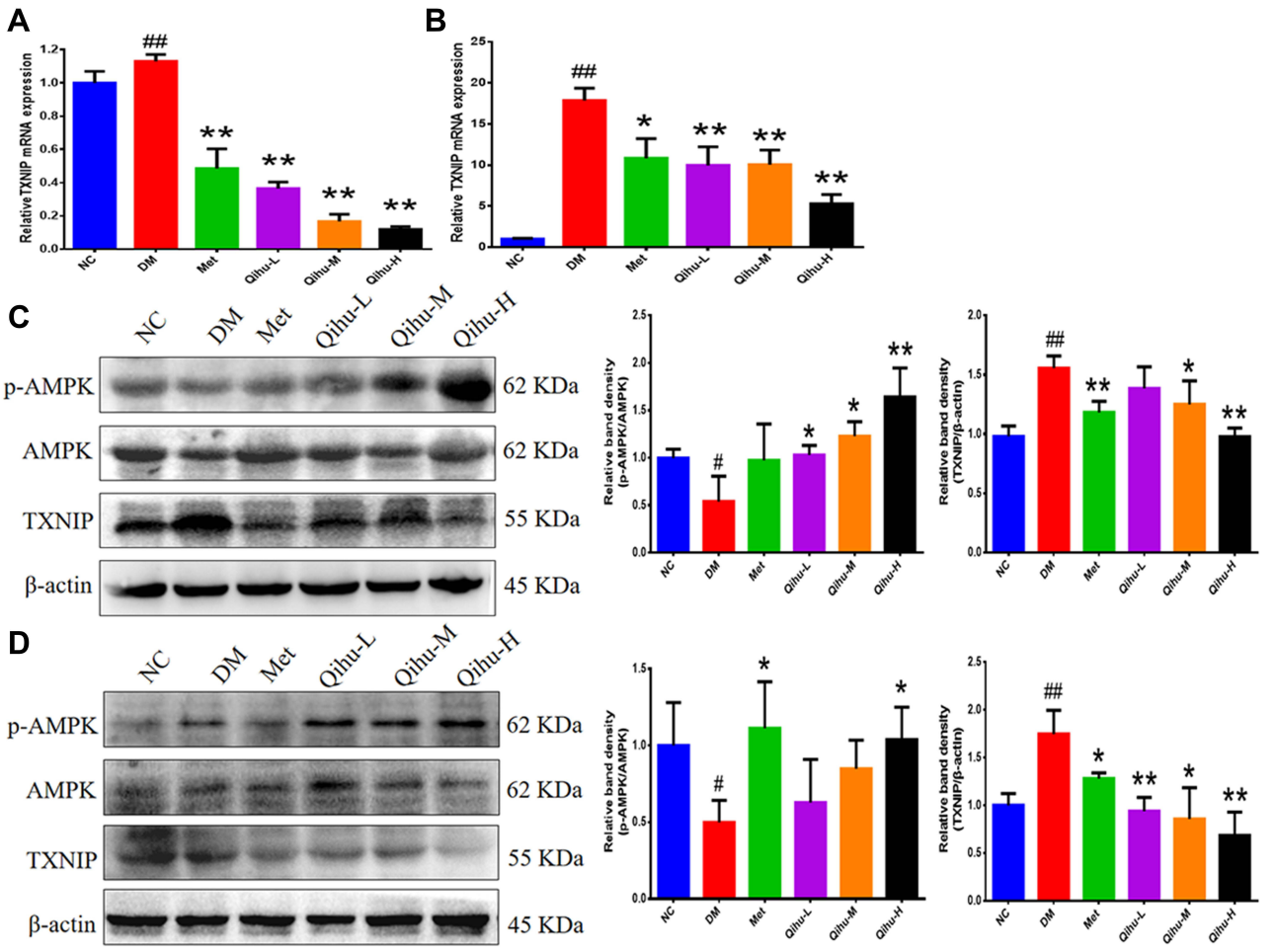

Figure 6 The effect of Qihu on AMPK signaling and TXNIP expression in the liver and pancreas of db/db mice. (**A** and **B**) The TXNIP mRNA levels in the liver (**A**) and pancreas (**B**) were detected by qRT-PCR assay. All data were expressed as mean ± SD (n = 3). (**C** and **D**) The protein levels of p-AMPK, AMPK and TXNIP in the liver (**C**) and pancreas (**D**) were detected by Western blot assay. The left panel is the representative Western blot result, and the right panel is the quantitative result of Western blot. $^{\#}p < 0.05$ or $^{\#\#}p < 0.01$ vs NC, $^{*}p < 0.05$ or $^{**}p < 0.01$ vs DM.

hyperlipidemia, fatty liver, and cirrhosis. Obesity, which is the main cause of metabolic disorders, decreases insulin sensitivity and adversely affects pancreatic cell function.[29] Compared with the DM group, the Qihu-M and Qihu-H groups exhibited significantly lower TG levels and lesser hepatocyte swelling and fat deposition. This indicated that Qihu can alleviate the pathological changes of the liver in db/db mice. The kidney and pancreas of the DM group did not exhibit pathological changes at the end of the experimental period. Hence, the effect of Qihu on kidney complications in db/db mice could not be determined in this study.

AMPK, a serine/threonine protein kinase, is an important drug target for metabolic syndrome and diabetes as it regulates cellular energy metabolic homeostasis. Previous studies have reported that AMPK can maintain cell function by promoting glycolysis and enhance the absorption of glucose by activating cell membrane vesicles containing GLUT4, which leads to the transport of glucose to the muscle membrane.[30] Jaiswal et al demonstrated that activating AMPK under metabolic stress can promote glucose uptake, inhibit fatty acid synthesis, and improve insulin sensitivity.[31] Recent studies have reported that upregulating the AMPK pathway can activate the NRF2/KEAP1 pathway, which leads to the alleviation of insulin resistance and diabetes-related complications induced by oxidative stress and inflammation.[32,33] TXNIP, also known as vitamin D3-upregulated gene 1 (VDUP1), plays a critical role in diabetes. Various epidemiological studies have demonstrated that the levels of TXNIP in patients with hyperlipidemia and hyperglycemia are significantly higher than those in healthy individuals.[34] The protein levels of TXNIP are upregulated in a mouse model of insulin resistance.[35] Shalev et al used gene chip technology and demonstrated that high glucose

levels can significantly upregulate TXNIP expression in the pancreatic β-cells.[36] AMPK can downregulate the TXNIP levels by promoting the degradation of TXNIP through the proteasome pathway.[37] Li et al reported that naringin can alleviate the inflammation in the gestational diabetes mellitus mouse model by activating the AMPK signaling pathway.[38] Hou et al reported that CD36 knockdown upregulated the AMPK activity and consequently inhibited the activation of NLRP3 inflammasomes and downregulated IL-1β secretion.[39] The overexpression of TXNIP can impair the cellular antioxidant defense mechanism, induce the release of proinflammatory mediators, such as TNF-α or IL-1β, and promote cell cycle arrest and apoptosis. Nyandwi et al demonstrated that rosmarinic acid can inhibit the assembly and activation of NLRP3 inflammasomes and decrease the secretion of IL-1β by downregulating the p38-FOXO1-TXNIP pathway in diabetic atherosclerosis.[40] Additionally, the enhanced glucose levels can upregulate the mRNA levels of IL-1β and promote insulin resistance through the upregulation of TXNIP in the human and mouse adipose tissue.[41] In this study, Qihu activated the AMPK signaling pathway and downregulated Txnip expression in the pancreas and liver tissues of db/db mice. Moreover, Qihu significantly downregulated the mRNA and protein levels of IL-1β and IL-6 in the pancreas and liver tissues of db/db mice.

Thus, Qihu can activate the AMPK signaling pathway, inhibit TXNIP expression, and suppress the secretion of inflammatory factors (IL-1β and IL-6) in db/db mice.

Conclusion

Qihu effectively decreased the blood glucose levels and alleviated histopathological changes in the liver of db/db mice. The anti-diabetic mechanism of Qihu in db/db mice involves the activation of the AMPK/TXNIP signaling pathway and the downregulation of inflammatory factor secretion.

Funding

This research was funded by Chongqing Municipal Science and Technology Commission of social undertakings and people's livelihood science and technology innovation special project (cstc2017shmsA0876), the Science and Technology Project of Chongqing Municipal Education Commission (grant number KJQN201800431), Basic Research and Frontier Exploration Project of Yuzhong District of Chongqing (grant number 20190102), Subject Talent Training Program of College of Pharmacy of Chongqing Medical University (grant number YXY2019XKDT2) and Chick Eagle Project of Chongqing Education Commission (grant number CY210411).

Disclosure

Weiying Zhou is a scientific consultant of Qihu Biopharmaceutical, reports grants from Chongqing Municipal Science and Technology Commission, Chongqing Municipal Education Commission, and Chongqing Medical University, during the conduct of the study, non-financial support from Qihu Biopharmaceutical, outside the submitted work, and no other potential conflicts of interest for this work. The other authors declare no conflicts of interest for this work.

References

1. Carracher A, Marathe P, Close K. International Diabetes Federation 2017. *J Diabetes*. 2018;10:353–356. doi:10.1111/jdb.12644
2. Flannick J, Johansson S, Njølstad P. Common and rare forms of diabetes mellitus: towards a continuum of diabetes subtypes. *Nat Rev Endocrinol*. 2016;12(7):394–406. doi:10.1038/nrendo.2016.50
3. Wu W, Hou J, Long H, Yang W, Liang J, Guo D. TCM-based new drug discovery and development in China. *Chin J Nat Med*. 2014;12:241–250.
4. Liu M, Liu Z, Xu B, Zhang W, Cai J. Review of systematic reviews and Meta-analyses investigating Traditional Chinese Medicine treatment for type 2 diabetes mellitus. *J Tradit Chin Med*. 2016;36:555–563. doi:10.1016/s0254-6272(16)30074-7
5. Zhang Q, Peng W, Wei S, et al. Guizhi-Shaoyao-Zhimu decoction possesses anti-arthritic effects on type II collagen-induced arthritis in rats via suppression of inflammatory reactions, inhibition of invasion & migration and induction of apoptosis in synovial fibroblasts. *Nat Rev Endocrinol*. 2019;118:109367.
6. Chen Z, Li J, Liu J, et al. Saponins isolated from the root of Panax notoginseng showed significant anti-diabetic effects in KK-Ay mice. *Am j Chinese Med*. 2008;36:939–951. doi:10.1142/S0192415X08006363
7. Yang C, Wang J, Zhao Y, et al. Anti-diabetic effects of Panax notoginseng saponins and its major anti-hyperglycemic components. *J Ethnopharmacol*. 2010;130:231–236. doi:10.1016/j.jep.2010.04.039
8. Li M, Zhang B, He S, Zheng R, Zhang Y, Wang Y. [Elucidating hypoglycemic mechanism of Dendrobium nobile through auxiliary elucidation system for traditional Chinese medicine mechanism]. *Chin J Chin Mater Med*. 2015;40:3709–3712. Chinese.
9. Teixeira da Silva J, Ng T. The medicinal and pharmaceutical importance of Dendrobium species. *Appl Microbiol Biotechnol*. 2017;101:2227–2239. doi:10.1007/s00253-017-8169-9
10. Commission. NP. *Pharmacopoeia of the People's Republic of China: I*. Beijing, China: China Medical Science and Technology Press; 2015.
11. Zhang X, Zhang B, Zhang C, Sun G, Sun X. Panax notoginsengEffect of Saponins and Major Anti-Obesity Components on Weight Loss. *Front Pharmacol*. 2020;11:601751. doi:10.3389/fphar.2020.601751
12. Yang Q, Wang P, Cui J, Wang W, Chen Y, Zhang T. Panax notoginseng saponins attenuate lung cancer growth in part through modulating the level of Met/miR-222 axis. *J Ethnopharmacol*. 2016;193:255–265. doi:10.1016/j.jep.2016.08.040
13. Hu S, Liu T, Wu Y, et al. Panax notoginseng saponins suppress lipopolysaccharide-induced barrier disruption and monocyte adhesion on bEnd.3 cells via the opposite modulation of Nrf2 antioxidant and NF-κB inflammatory pathways. *Phytother Research*. 2019;33(12):3163–3176. doi:10.1002/ptr.6488

14. He T, Huang Y, Yang L, et al. Structural characterization and immunomodulating activity of polysaccharide from Dendrobium officinale. *Biol Macromol*. 2016;83:34–41. doi:10.1016/j.ijbiomac.2015.11.038
15. Ke Y, Zhan L, Lu T, et al. Dendrobium officinalePolysaccharides of Kimura & Migo Leaves Protect Against Ethanol-Induced Gastric Mucosal Injury the AMPK/mTOR Signaling Pathway and. *Front Pharmacol*. 2020;11:526349. doi:10.3389/fphar.2020.526349
16. Zhu Y, Liu M, Cao C, et al. Dendrobium officinale flos increases neurotrophic factor expression in the hippocampus of chronic unpredictable mild stress-exposed mice and in astrocyte primary culture and potentiates NGF-induced neuronal differentiation in PC12 cells. *Phytother Research*. 2021:1–13. doi: 10.1002/ptr.7013.
17. Zhang K, Zhou X, Wang J, et al. Dendrobium officinale polysaccharide triggers mitochondrial disorder to induce colon cancer cell death via ROS-AMPK-autophagy pathway. *Carbohydr Polym*. 2021;264:118018. doi:10.1016/j.carbpol.2021.118018
18. Zhang X, Li X, Wang N, Yao X, Zhou W. Pharmacodynamics of Qihu preparations for treatment of diabetes in mice. *J Third Military Med Univ*. 2017;39:1422–1427. doi:10.16016/j.1000-5404.201612006
19. Li X, Zhu G, Yao X, et al. Celastrol induces ubiquitin-dependent degradation of mTOR in breast cancer cells. *Onco Targets Ther*. 2018;11:8977–8985. doi:10.2147/OTT.S187315
20. Coughlan K, Valentine R, Ruderman N, Saha A. Nutrient Excess in AMPK Downregulation and Insulin Resistance. *J Endocrinol, Diabetes Obesity*. 2013;1:1008.
21. Salminen A, Hyttinen J, Kaarniranta K. AMP-activated protein kinase inhibits NF-κB signaling and inflammation: impact on healthspan and lifespan. *J Mol Med*. 2011;89:667–676. doi:10.1007/s00109-011-0748-0
22. Parikh H, Carlsson E, Chutkow W, et al. TXNIP regulates peripheral glucose metabolism in humans. *PLoS Med*. 2007;4:e158. doi:10.1371/journal.pmed.0040158
23. Zhang Q, Pan Y, Wang R, et al. Quercetin inhibits AMPK/TXNIP activation and reduces inflammatory lesions to improve insulin signaling defect in the hypothalamus of high fructose-fed rats. *J Nutr Biochem*. 2014;25:420–428. doi:10.1016/j.jnutbio.2013.11.014
24. Sharma B, Kim H, Rhyu D. Caulerpa lentillifera extract ameliorates insulin resistance and regulates glucose metabolism in C57BL/KsJ-db/db mice via PI3K/AKT signaling pathway in myocytes. *J Transl Med*. 2015;13:62. doi:10.1186/s12967-015-0412-5
25. Xu J, Wang S, Feng T, Chen Y, Yang G. Hypoglycemic and hypolipidemic effects of total saponins from Stauntonia chinensis in diabetic db/db mice. *J Cell Mol Med*. 2018;22:6026–6038. doi:10.1111/jcmm.13876
26. Zhuang M, Qiu H, Li P, Hu L, Wang Y, Rao L. Edgeworthia gardneriIslet protection and amelioration of type 2 diabetes mellitus by treatment with quercetin from the flowers of. *Drug Des Devel Ther*. 2018;12:955–966. doi:10.2147/DDDT.S153898
27. Guo X, Sun W, Luo G, et al. Panax notoginseng saponins alleviate skeletal muscle insulin resistance by regulating the IRS1-PI3K-AKT signaling pathway and GLUT4 expression. *FEBS Open Bio*. 2019;9:1008–1019. doi:10.1002/2211-5463.12635
28. Tang H, Zhao T, Sheng Y, Zheng T, Fu L, Zhang Y. Dendrobium officinale Kimura et Migo: a Review on Its Ethnopharmacology, Phytochemistry, Pharmacology, and Industrialization. *Evidence-Based Compl Alternative Med*. 2017;2017:1–19. doi:10.1155/2017/7436259
29. Kumar S, Behl T, Sachdeva M, et al. Implicating the effect of ketogenic diet as a preventive measure to obesity and diabetes mellitus. *Life Sci*. 2021;264:118661.
30. Lin S, Hardie D. AMPK: sensing Glucose as well as Cellular Energy Status. *Cell Metab*. 2018;27(2):299–313. doi:10.1016/j.cmet.2017.10.009
31. Jaiswal N, Gavin M, Quinn W, et al. The role of skeletal muscle Akt in the regulation of muscle mass and glucose homeostasis. *MOL METAB*. 2019;28:1–13. doi:10.1016/j.molmet.2019.08.001
32. Gupta A, Behl T, Sehgal A, Bhatia S, Jaglan D, Bungau S. Therapeutic potential of Nrf-2 pathway in the treatment of diabetic neuropathy and nephropathy. *Mol Biol Rep*. 2021;48(3):2761–2774. doi:10.1007/s11033-021-06257-5
33. Behl T, Kaur I, Sehgal A, et al. Unfolding Nrf2 in diabetes mellitus. *Mol Biol Rep*. 2021;48(1):927–939. doi:10.1007/s11033-020-06081-3
34. Zhao Y, Li X, Tang S. Retrospective analysis of the relationship between elevated plasma levels of TXNIP and carotid intima-media thickness in subjects with impaired glucose tolerance and early Type 2 diabetes mellitus. *Diabetes Res Clin Pract*. 2015;109:372–377. doi:10.1016/j.diabres.2015.05.028
35. Sun H, Hu Y, Zhao X, et al. Age-related changes in mitochondrial antioxidant enzyme Trx2 and TXNIP-Trx2-ASK1 signal pathways in the auditory cortex of a mimetic aging rat model: changes to Trx2 in the auditory cortex. *FEBS J*. 2015;282:2758–2774. doi:10.1111/febs.13324
36. Shalev A, Pise-Masison C, Radonovich M, et al. Oligonucleotide microarray analysis of intact human pancreatic islets: identification of glucose-responsive genes and a highly regulated TGFbeta signaling pathway. *Endocrinology*. 2002;143:3695–3698. doi:10.1210/en.2002-220564
37. Wu N, Zheng B, Shaywitz A, et al. AMPK-dependent degradation of TXNIP upon energy stress leads to enhanced glucose uptake via GLUT1. *Mol Cell*. 2013;49:1167–1175. doi:10.1016/j.molcel.2013.01.035
38. Li S, Zhang Y, Sun Y, et al. Naringenin improves insulin sensitivity in gestational diabetes mellitus mice through AMPK. *Nutr Diabetes*. 2019;9(1):28. doi:10.1038/s41387-019-0095-8
39. Hou Y, Wang Q, Han B, et al. CD36 promotes NLRP3 inflammasome activation via the mtROS pathway in renal tubular epithelial cells of diabetic kidneys. *Cell Death Dis*. 2021;12(6):523. doi:10.1038/s41419-021-03813-6
40. Nyandwi J, Ko Y, Jin H, Yun S, Park S, Kim H. Rosmarinic acid inhibits oxLDL-induced inflammasome activation under high-glucose conditions through downregulating the p38-FOXO1-TXNIP pathway. *Biochem Pharmacol*. 2020;182:114246. doi:10.1016/j.bcp.2020.114246
41. Koenen T, Stienstra R, van Tits L, et al. Hyperglycemia activates caspase-1 and TXNIP-mediated IL-1beta transcription in human adipose tissue. *Diabetes*. 2011;60:517–524. doi:10.2337/db10-0266